An Evaluation of Current Ship Wake Detection Algorithms in SAR Images

Andreas Arnold-Bos, Ali Khenchaf, Arnaud Martin
Laboratoire E^3I^2, Ecole Nationale Supérieure des Ingénieurs et Techniques de l'Armement, 2 rue François Verny, 29200 Brest CEDEX, France
E-mail: {`arnoldan,khenchal,martinar`}`@ensieta.fr`

SHORT ABSTRACT: *Ship wakes are often used as the primary means to detect ships in SAR images since they can extend for kilometers. On radar images, they often take the appearance of bright and/or dark lines hidden in the sea clutter. For this reason, robust and efficient line detection algorithms are needed. Our first results tend to support the classical method relying on the Radon Transform and confirm the improvements brought the recently proposed stochastic matched filtering (proposed in 2005), but are somewhat mitigated about the wavelet correlator (proposed in 2003), the Hough Transform or the use of Wiener filtering to improve the Radon Transform thresholding.*
Keywords: *ship wakes, radar, SAR, line detection.*

RÉSUMÉ COURT: *Le sillage est considéré comme l'une des signatures les plus significatives d'un navire dans une image radar, car il peut s'étendre sur plusieurs kilomètres. Il prend la forme de lignes sombres et/ou claires qui sont noyées dans le fouillis de mer. Pour cette raison, des algorithmes de détection de ligne robustes sont nécessaires. Nos premiers résultats tendent à soutenir la méthode classique fondée sur la transformée de Radon et confirment l'efficacité du filtrage stochastique adapté (proposé en 2005), mais sont mitigés au sujet de la corrélation intra-échelle de la transformée en ondelette (proposée en 2003), de la transformée de Hough, ou de l'utilisation du filtrage de Wiener pour améliorer le seuillage de la transformée de Radon.*
Mots-clés: *sillages, radar, ROS, détection de droites.*

1 INTRODUCTION

Ship wakes are often used as a primary means of detecting a ship in synthetic aperture radar (SAR) images since they last for often many hours, thus leaving a trail that can extend for kilometers. The image of the wake is larger than the echo of the ship itself and is generally visible from space. The wake has the added advantage of providing information on the heading of the ship. Furthermore, if the image resolution is good enough, additional parameters can be extracted from the wake, such as the beam of the ship and its speed [1]. That information can be fed as an input to ship tracking or ship identification algorithms.

The appearance of wakes in radar images depends on various parameters [2]: the shape of the hull – as mentioned above – but also on the sea state, the observation geometry and the characteristics of the radar, like the carrier frequency, the polarization, or the observation configuration (monostatic or bistatic). Depending on the configuration, one or several of the following features are visible. First, the wake is nearly always characterized by a dark streak behind ships. This dark trail originates from the turbulent vortex created by the ship, which reduces the roughness of the sea. The dark wake may be delimited by one or two bright lines, especially in L-band radar. Sometimes also, often in X-band radar, another set of bright arms can be visible: they are located at the border of the Kelvin wavesystem and form a characteristic angle of about 39°. **Fig. 3.a** presents a ERS-1 C-band image of a ship where the dark turbulent wake and a bright Kelvin arm are clearly visible.

These two sets of features (dark lines, bright lines) are of primary importance when wake detection is considered, because they allow for the use of *line detection algorithms*. However, the detection task is complicated by the presence of multiplicative noise (speckle), which is prominent when the sea state is high, since it hides the wake. This paper analyzes and compares existing methodologies to deal with automatic ship wake detection in SAR images.

In section 2, we carry out a review of existing methodologies. We focus our analysis on four approaches in particular, which we feel are representative of the spectrum of methods available today. Most of the algorithms reviewed here begin with the Radon transform, since its properties make it particularly suitable to line detection in speckle noise. The Radon transform is applied to the raw, noisy image, and the features visibility is then optimized by using subsequent processing stages such as *i)* Wiener filtering [3] or *ii)* the stochastic matched filtering method, which has been proposed recently [4]. Other approaches relie on multiscale analysis, such as *iii)* wavelet transforms [5]. Those extract features by assuming that objects such as wakes display a certain correlation between adjacent scales, unlike noise. Finally, another approach may be to use *iv)* the Hough transform [6], which is related to the Radon transform in its principle and can be faster to compute, but which is not as robust to noise; that third approach requires to despeckle the image beforehand.

Section 3 presents a comparison of these methods, both on actual data, and on simulated images. The criteria we used are the computation complexity, the computation time, and a first evaluation of the robustness to noise.

2 DESCRIPTION OF THE ALGORITHMS

Wake detection generally follows the process outlined in **Fig. 1**. First, it can begin by an optional pre-processing step. This stage aims at reducing the amount of speckle while preserving, or even enhancing, the visibility of the wake features. Then, a transform is performed, so as to reduce the dimension of the problem. Another parametrization is used to represent a line: instead of representing it by the collection of pixels which form its image, an analytic representation is preferred. Lines are represented by the reduced equation $\rho = x.\cos\theta + y.\sin\theta$ where $\rho \in \mathbb{R}$ is the distance of the line to the origin of the image, and $\theta \in [0; \pi[$ the angle between the normal to the line, and the x axis. The line can thus be represented by the couple (ρ, θ), that is, a single point in a radius-angle plane. The problem is then to transform the image from the (x, y) plane into a representation in the radius-angle plane. A computer representation of the radius-angle plane requires however that plane to be quantized in bins of size $\Delta\theta \times \Delta\rho$. Two methods are commonly used: the Radon Transform (RT) and the Hough Transform (HT). The RT or HT must then be adequately thresholded to isolate those points (ρ, θ) that correspond to a line in the image. So as to increase the signal-to-noise ratio in the radius-angle space, the thresholding is often preceded by another cleaning step.
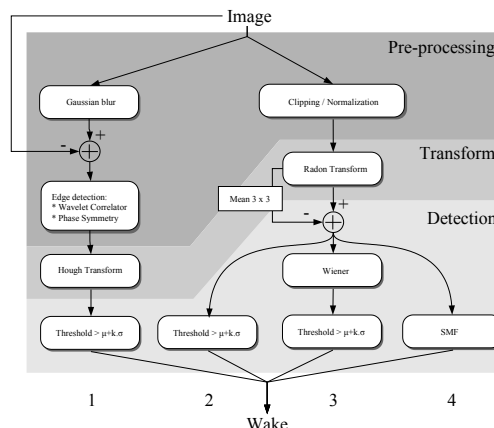
Fig. 1: Flowchart of the four algorithms {1, 2, 3, 4} presented in this paper

2.1 The Radon Transform and the Hough Transform

The Radon Transform of image I is defined in such a way that the value of the transform at (ρ_0, θ_0), is equal to the integral of the image over the line of equation $\rho_0 = x.\cos\theta_0 + y.\sin\theta_0$. Mathematically, this representation can be written:

$$RI(\rho_0, \theta_0) = \iint_{x,y} I(x,y)\delta_0(x.\cos\theta_0 + y.\sin\theta_0 - \rho_0) \tag{1}$$

This transformation is invertible. If x_0 and y_0 are fixed, then the sum over the sinusoid of equation $\rho = x_0.\cos\theta + y_0.\sin\theta$ in the Radon plane will yield the intensity of the pixel at coordinates (x_0, y_0) in the image plane. The Radon Transform is generally not used for line detection but it is well-adapted to that task for images of the sea. Ship wakes are either very bright or very dark, while the sea returns are average. Intuitively, if all the pixels of a given line are bright, and the others are only average, the Radon Transform of the image will bring a large sum at the particular (ρ, θ) point corresponding to the line, and moderate values elsewhere. Said otherwise, a spike appears at point (ρ, θ). A simple thresholding of the Radon Transform will then allow the user to detect that particular point and provide the analytical representation of the line. A dark line will similarly yield a strong negative spike. On the other hand, through summing, speckle is somewhat canceled.

The Hough Transform was introduced in a patent by Paul Hough in 1966 and also uses a parametric representation of a line. Initially, the $y = a.x + b$ parametrization was used, with is problematic for vertical lines since a becomes infinite. Duda & Hart [7] suggested using the same parametrization as the Radon Transform, which is how the Hough Transform for lines is mainly known as today. Before computing a Hough Transform, an edge detector is applied to the image; this can be seen as a particular cleaning step as exposed above, since highlighting edges already requires to cast out the noise. A binary edge map is obtained: a particular pixel at (x_0, y_0) has a value of 0 if the pixel is not located on an edge, 1 otherwise. Since pixel (x_0, y_0) can belong to an infinity of lines having an equation of the form: $\rho = x_0.\cos\theta + y_0.\sin\theta$, which is a sinusoid in the $\rho - \theta$ space, all bins of the radius-angle plane that intersect it are incremented by one in a process known as "voting". All in all, if many pixels are located in the image space on a line of equation $\rho_0 = x.\cos\theta_0 + y.\sin\theta_0$, the corresponding (ρ_0, θ_0) bin will have a large number of votes. Again, thresholding the Hough transform yields the parametric representation of the lines in the image. Contrarily to the Radon Transform, the Hough Transform is not strictly invertible.

2.2 Image enhancement prior to transforming

Denoising & improved edge detection Radar images are corrupted by speckle. This is a cause for concern when detecting the wake features, since speckle makes them less visible and harder to detect. This is especially true when the Hough Transform is to be used, since the edges must be perfectly detectable and noise must not be considered as an edge. Classical edge detectors such as the Canny-Deriche filter [8] behave poorly in heavily speckled images: the Canny detector, which is linear, smooths the image at the same time it performs detection but in an indiscriminate way, thus dampening the image gradient near edges when too much smoothing is needed. Adaptive filters, often based on wavelets, have been shown to be more suited to perform denoising; a good example might be the Enriched Diversity Digital Wavelet Transform [9]. Instead of using the image gradient to detect edges, other criteria that are more robust to noise can be used. In our case, we used the phase symmetry from Kovesi [10]. When the image is moderately unspeckled, or after applying a median filter, phase symmetry allows for detecting the line sufficiently well enough so that the Hough transform may be applied.

The Wavelet Correlator The use of an intra-scale correlation on the wavelet decomposition of the image has been proposed by Kuo and Chen [5] with the intent of enhancing the visibility of the edge-like features of wakes prior to computing the Radon Transform or the Hough Transform. The idea is to compute a Discrete Wavelet Transform (DWT) of the image on n scales, which yields for each scale four sub-images: the approximation A_j, and three detail images D_j^h, D_j^v and D_j^d (horizontal, vertical and diagonal details). As a side-effect, the dimensions of the sub-images at scale j are reduced by a factor 2^{-j} compared to the original size. Then, the modulus of the detail

image is computed at each scale j:

$$M_j = \sqrt{|D_j^h|^2 + |D_j^v|^2 + |D_j^d|^2} \tag{2}$$

A wavelets correlation for the image at position (x, y) is computed by multiplying the moduli M_j for which the point at (x, y) has contributed, over all scales (this requires to re-sample the M_j, $j > 1$ images to the same size as M_1, which we symbolize by the $[\uparrow 2^x]$ operator):

$$R = \prod_{j=1}^{n} [\uparrow 2^{j-1}] M_j \tag{3}$$

2.3 Thresholding in the $\rho - \theta$ space

Direct thresholding   Once the Radon or the Hough Transform are computed, the spikes corresponding to the lines must be detected. In the approach proposed by Rey *et al.* [3], the running mean (computed on a 3×3 window) of the Radon transform, is subtracted to it, so as to enhance the visibility of the spikes corresponding to the lines. **Fig. 2** shows the result of that operation on a sample image. Then, the standard deviation of the Radon Transform σ is computed, and each bin that has a modulus greater than $k \times \sigma$ ($k \approx 3 - 4$) is considered as a spike.

Thresholding after Wiener filtering   Since the digital Radon Transform is computed on bins, of width $\Delta \rho \times \Delta \theta$, and since the lines have a given width which is not necessarily zero, it so occurs that the spike corresponding to a line in the Radon Transform is not a Dirac and spills over on adjacent bins. Rey *et al.* [3] proposed to model the spike as a Gaussian, and advocated the use of Wiener filtering to increase the sharpness of the spike. Basically, everything happens as if the Radon Transform (which admits R as a Fourier Transform) were the blurred version of some ideal image (which has R' as its Fourier Transform) where the spikes are pure Diracs. The transfer function is a Gaussian kernel H, and the background signal (Fourier Transform: N) is considered as noise: $R = H.R' + N$. Using Wiener filtering aims at estimating R' by inverting the blurring process to retrieve the Dirac without the noise level being increased too much during the inversion process. If $\bar{R}$ is the Fourier Transform of the estimate:

$$\bar{R} = \frac{H^\star}{|H|^2 + \lambda} R \tag{4}$$

with λ chosen as the noise-to-signal ratio.

The Stochastic Matched Filter   The Stochastic Matched Filter (SMF) can be seen as an extension of the traditional matched filter. The matched filter is the optimal linear optimal filter under the following hypotheses: *i*) the useful signal to detect is perfectly known and *ii*) the noise is additive. The use of SMF for wake detection has been proposed by Courmontagne in [4].

Let Z be the observed signal: $Z = S + N$, where S is the useful signal and N the noise. Z is sampled on n values $Z(1)$ to $Z(n)$. We call $W(s)$ a window of width $L = 2l + 1$ centered around sample s: $W(s) = [Z(s - 2l), ..., Z(s), ..., Z(s + 2l)]^t$. $W(s)$ is the sum of two random vectors $W_S(s)$ and $W_N(s)$ representing respectively the windowed sequence of useful signal samples and the windowed sequence of noise samples. $W(s)$, $W_S(s)$ and $W_N(s)$ can be modeled as random vectors taking values in the gray levels space; let G be the number of possible gray values. There are G^L different manners to construct a realization of a window $W(s)$. We note p_i the probability of observing configuration W_S^i of $W_S(s)$ and q_j the probability of observing configuration W_N^j of the noise. Thus, the average signal to noise ratio on window $W(s)$ before filtering is:

$$\text{SNR}(s) = \frac{\sum_{i=1}^{G^L} p_i . W_S^{i\,t} . W_S^i}{\sum_{j=1}^{G^L} q_j . W_N^{j\,t} . W_N^j} \tag{5}$$

The stochastic matched filter is a FIR filter H of length L which is intended to maximize the signal-to-noise ratio after filtering, which we note SNR':

$$\text{SNR}'(s) = \frac{\sum_{i=1}^{G^L} p_i . (H^t.W_S^i)^t . (H^t.W_S^i)}{\sum_{j=1}^{G^L} q_j . (H^t.W_N^j)^t . (H^t.W_N^j)} = \frac{H^t . \left(\sum_{i=1}^{G^L} p_i . W_S^i . W_S^{i\,t} \right) . H}{H^t . \left(\sum_{j=1}^{G^L} q_j . W_N^j . W_N^{j\,t} \right) . H} = \frac{H^t . \Gamma_S . H}{H^t . \Gamma_N . H} \tag{6}$$

Γ_S and Γ_N are the covariance matrices of $W_S(s)$ and $W_N(s)$, respectively. We can write $A = \Gamma_S/\text{trace}(\Gamma_S)$ and $B = \Gamma_N/\text{trace}(\Gamma_N)$, thus we get:

$$\text{SNR}'(s) = \frac{\text{trace}(\Gamma_S)}{\text{trace}(\Gamma_N)} \cdot \frac{H^t.A.H}{H^t.B.H} \tag{7}$$

The theory shows that the SNR is improved when H is an eigenvector X_i of $C = B^{-1}.A$ associated to an eigenvalue $\lambda_i > 1$, and the improvement ratio is λ_i, if the eigenvector is normalized such that $X_i^t.B.X_i = 1$. There are $Q \leq L$ eigenvectors associated to eigenvalues greater than one. This result can be used in two ways:

1. To enhance the observed signal: an enhanced version of $W(s)$ would be:

$$W'(s) = \sum_{i=1}^{i \leq Q} H_i^t.W(s)$$

2. To detect whether the signal is present or absent, by computing a threshold with which the wake signature can be detected using a maximum likelihood scheme [4].

Using the stochastic matched filter requires to decompose C into eigenvectors, and thus to know Γ_S and Γ_N. Γ_S is modeled *a priori* on a large number of simulations of the useful signal in a noise-free environment. This matrix will have a size $L \times L$. The number of simulations must be larger than L to prevent the covariance matrix from being nearly singular. Similarly, the covariance matrix of W_N is obtained on more than L simulations or examples of W_N (taken from the observation when the absence of useful signal is guaranteed). This can be partly done off-line. When the signal to detect is perfectly known, C has only one eigenvector which is the mirrored, conjugate version of that signal, and we fall back to the traditional matched filter theory.

In the case of a 2-D signal, $W(s)$ can be constructed by taking a 2-D window, then concatenating all the lines of the window to form a 1-D vector. The 1-D theory is used, then the 2-D filters are retrieved by folding back the X_i's into 2-D masks. Two-dimensional correlations can also be used [11].

3   COMPARISON OF THE METHODS

We implemented four algorithms, as indicated in **Fig. 1**, which make use of the aforementioned methods in a coherent way, while bearing in mind that in some cases, some stages could be swapped between some algorithms. In algorithm 1, the first stage consists in subtracting the local average of the image to make it more robust to local variations of intensity of the image. Either the Wavelet Correlator, or the Phase Symmetry algorithm is used in the pre-processing. The second and third algorithm are our own direct implementation of the algorithms proposed by Rey *et al*. The fourth one is our own interpretation of the stochastic adapted filter.

3.1   Computation complexity

All the linear filtering operations except the DWT are computed using a FFT. For an image of size $N \times N$, this yields a $\mathcal{O}(N \log N)$ complexity. The complexity of the DWT, when Mallat's algorithm is used, is in $\mathcal{O}(N^2)$. The computation of the Radon Transform for an $N \times N$ image over M angles (where M has the same order as N) has a $\mathcal{O}(N^2.M) \approx \mathcal{O}(N^3)$ complexity in its simplest form though a parallel algorithm exists that brings the complexity down to $\mathcal{O}(N^2.\log N)$ [12]. The Hough Transform has a $\mathcal{O}(N^2.M)$ complexity too, but since it works on binarized images where not all the points contribute, its computation time is marginally lower than the Radon Transform. However, the intensive preprocessing required by the Hough Transform can add a tremendous computation cost. A special note must be given about the Stochastic Matched Filtering: while the Matched Filtering phase itself can be computed using a series of FFT (one per H_i), the preparation phase takes more time. As we implemented it, the filter is applied on a 17×17 window, which requires the computation of two 289×289 covariance matrices. In particular, computing the covariance matrix of the signal requires to simulate the appearance of several line signatures in the Radon plane, which means performing as many Radon Transforms (in our case, more than 289; otherwise, the covariance matrix would be nearly singular and some eigenvalues infinite).

3.2 Computation time

The key computation times are the following: while Algorithm 2 and 3 are nearly instantaneous, since the only long stage is the Radon transform (1 second, typically, with the optimized Matlab routine on a Pentium IV), computing Γ_S takes about 1500 s for 512 trials (and as many Radon transforms); this can however be done off line. Computing Γ_N takes only 89 s since only one Radon Transform needs to be computed: that of the image to filter, from which the noise information is extracted. The phase symmetry algorithm takes about four seconds to compute under Matlab, and the Wavelet Correlator about two.
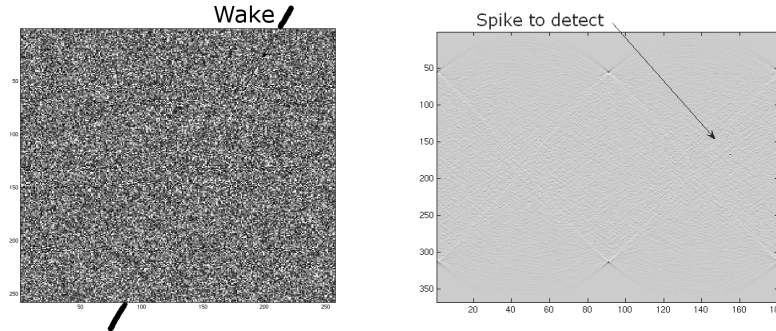
Fig. 2: "Simple Line Image 2" (SNR 2 dB), and its Radon Transform without the local mean

3.3 Comparison on images

We first compared the algorithms on a real image (fig. 3.a). Since all algorithms detected the wake satisfactorily with a good margin, we decided to test how the images behaved in a simple case with noise increasing. We generated four synthetic images (size 256×256) which were corrupted by Rayleigh noise (the image is not clipped at 255). The "simple line images" consist in two linear trails, one dark, and one bright, which is typical of the turbulent wake; each trail is one pixel large. The average sea return is set to gray level 128; the gray level of the wake varies in each image according to the following table (the values in dB are the relative differences with the mean sea return, which we call somewhat abusively the "image SNR"). When detecting, the thresholding parameters are set to wake detection limit..

Image	Dark arm	Bright arm	Difference (dB)
1	64	255	±3
2	81	203	±2
3	101	161	±1
4	114	144	±0.5

Algorithm 1 performs moderately well on low SNR. The Wavelets Correlator does not lock on linear features as well as expected, even if it highlights the ship in the real image really well (fig. 3.b). We explain this behavior by the following: wavelets are adapted to detect punctual singularities but not higher order ones, such as lines. The wavelets correlator performs better on higher resolution wakes, such as the SAR image obtained with the ENSIETA simulator [13] where the Kelvin wake system is clearly visible (fig. 4); this was also the configuration shown in the original paper by Kuo and Chen [5]. On the other hand, the phase symmetry detector provides sufficiently points for the Hough Transform to lock well. The downside is that this is rather (about 6 FFTs), which nullifies the gain in speed obtained with the Hough Transform. Nothing is detected below a 2 dB image SNR, because the edge detector fails to extract the wake.

Algorithm 2 and 3 behave well on all images when the SNR is reasonably high, but tend to raise false alarms when the signal-to-noise ratio decreases, or to falsely claim that no wake is present when there is one. Adding the Wiener filter is sometimes efficient, but requires a delicate tuning of the Gaussian used for deconvolution. Our experience is that detection is generally less robust with the Wiener filter than without (all other things remaining the same). This could be explained by the fact that deconvolution is not intended to augment the signal to noise ratio, but only to reduce the spike
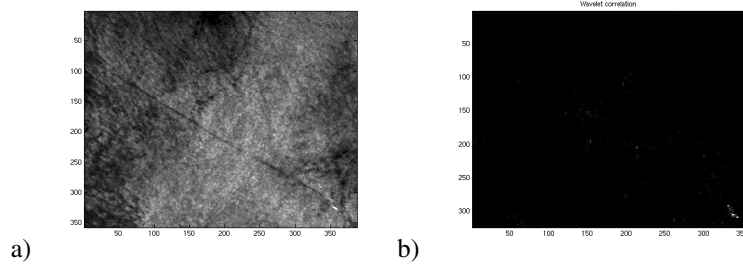
Fig. 3: a) ERS-1 image (© ESA), b) wavelet correlation on 4 scales. Notice how only the ship is detected by the wavelet correlation.
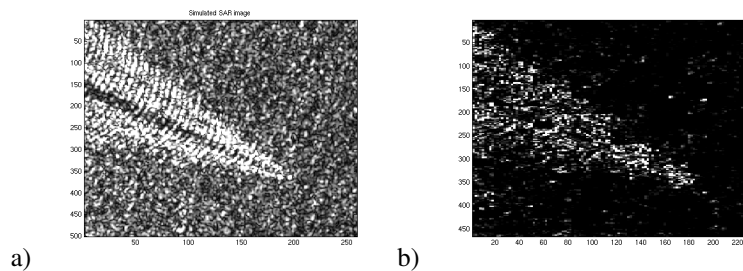
Fig. 4: a) simulated SAR image [13], $\approx 2 \times 2$ m resolution, sea state 2. b) result of the wavelet correlator on 5 scales.

width; besides, the Gaussian is only a crude approximation of the appearance of the wake spike in the Radon plane. Without the Wiener filter, algorithm 2 detects the wake without any false alarm for an image SNR equal to 1 (threshold set to $m + 9\sigma$); when the SNR drops to 0.5, the threshold fails to $m + 4.5\sigma$; the wake is detected but typically many false lines are detected, too (fig. 5.a).

Algorithm 4 (the stochastic matched filter) has the best results. The threshold remains relatively stable (about 0.7 times the maximum) as the SNR augments and at SNR = 0.5 dB, the number of falsely detected lines, at the detection limit of the real wake, is typically half the number of falsely detected lines obtained with algorithm 2 (fig. 5.b).

4 DISCUSSION & CONCLUSION

It appears that the Stochastic Adapted Filtering seems promising, and brings a little improvement in detection that comes at a cost: the signal must be modeled a priori through simulation. This can be done off- line, however. The classical algorithm comes second in our evaluation and has the merit of being simple and fast. The Hough Transform is too much unsuited for wake detection, since it requires a too intensive preprocessing step to be really interesting. Finally, our position on the the wavelet correlator is ambivalent: it does indeed highlight interesting features such as ships and removes the background noise (sea waves), but sometimes fails to capture linear features as desired; its use must probably be studied more. This paper is only but a first approach for a comparison of common wake detection algorithms. For a more thorough comparison of the algorithms, statistical measures must be performed. These would require typically a thousand realizations per given configuration (noise level, wake position & direction, presence or absence of wake), which understandably requires time, but this study is envisaged at the ENSIETA. The final step would be a benchmark on a bank of real images, where the algorithms outputs would be compared to several manual segmentations provided by human experts, for instance by resusing the metric introduced recently by two of us [14].

References

[1] G. Zilman, A. Zapolski, and M. Marom, "The speed and beam of a ship from its wake's SAR images," *IEEE Transactions on Geoscience and Remote Sensing*, vol. 42, Oct. 2004.
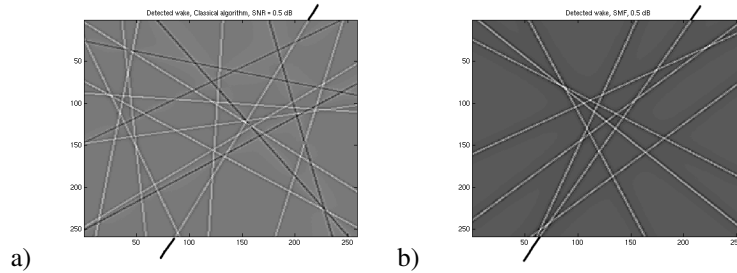
Fig. 5: Lines obtained at the detection limit of the true wake at SNR 0.5 dB. a): algorithm 2, b), algorithm 4.

[2] A. M. Reed and J. H. Milgram, "Ship wakes and their radar images," *Annual Review of Fluid Mechanics*, no. 34, pp. 469–502, 2002.

[3] M. T. Rey, J. K. Tunaley, J. T. Folinsbee, P. A. Jahans, J. A. Dixon, and M. R. Vant, "Application of Radon transform techniques to wake detection in Seasat-A SAR images," *IEEE Transactions on Geoscience and Remote Sensing*, vol. 28, July 1990.

[4] P. Courmontagne, "An improvement of ship wake detection based on the Radon transform," *Signal Processing*, vol. 85, no. 2005, pp. 1634–1654, 2005.

[5] J. M. Kuo and K.-S. Chen, "The application of wavelets correlator for ship wake detection in SAR images," *IEEE Transactions on Geoscience and Remote Sensing*, vol. 41, June 2003.

[6] J. Iisaka, J. H. Bloedow, and T. S. Amano, "Automatic detection of V-shaped features from SAR imagery," in *Proceedings of the Asian Conference on Remote Sensing*, 1996.

[7] R. O. Duda and P. E. Hart, "Use of the Hough transform to detect lines and curves in pictures," *Communications of the ACM*, vol. 15, no. 1, pp. 11–15, 1972.

[8] R. Deriche, "Using Canny's criteria to derive a recursively implemented optimal edge detector," *International Journal of Computer Vision*, vol. 1, no. 2, pp. 167–187, 1987.

[9] A. Isar, A. Quinquis, M. Legris, and D. Isar, "Débruitage des images sar : Application de la todde (transformée en ondelettes à diversité enrichie)," *RSTD Revue Scientifique et Technique de la Défense*, vol. 64, 2004.

[10] P. Kovesi, "Symmetry and asymmetry from local phase," in *Australian Joint Conference on Artificial Intelligence*, Dec. 1997.

[11] D. Zhang, S. Chen, and J. Liu, "Representing image matrices: Eigenimages vs. eigenvectors," in *International Symposium on Neural Networks*, vol. 2, 2005.

[12] M. T. Frederick, N. A. Van der Horn, and A. K. Somani, "Real-time hardware implementation of the approximate discrete radon transform," in *16th IEEE International Conference on Application-Specific Systems, Architectures, and Processors (ASAP 2005), Samos, Greece*, July 2005.

[13] A. Arnold-Bos, A. Martin, and A. Khenchaf, "A bistatic & polarimetric marine radar simulator," in *IEEE Conference on Radars (Verona, NY)*, Apr. 2006.

[14] A. Martin, H. Laanya, and A. Arnold-Bos, "Evaluation for uncertain image classification and segmentation," *Pattern Recognition*, vol. 39, pp. 1987–1995, Nov. 2006.